ELSEVIER

Wear 186–187 (1995) 360–367

WEAR

Water droplet erosion of laser surface treated Ti–6Al–4V

J.M. Robinson [1], R.C. Reed[1]

Department of Materials, Imperial College of Science, Technology and Medicine, London SW7 2BP, UK

Abstract

The work reports on the effect of laser surface treatments on the water droplet erosion resistance of a commercial alloy of nominal composition Ti–6Al–4V. Use is made of a continuous wave CO_2 laser to melt the Ti–6Al–4V in both inert and dilute nitrogen atmospheres. The gas composition of the atmosphere is set at either 100% Ar, 90% Ar + 10% N_2 or 80% Ar + 20% N_2 by volume. The successive intertrack overlap is set at either 50% or 75% of the surface width of a single melt track. The cumulative mass loss during water droplet erosion of the laser surface melted material decreases substantially relative to the untreated material for all processing conditions examined. The enhanced erosion resistance is attributed to increases in the surface layer microhardness as well as the resistance of the martensitic microstructure to the hydraulic penetration mechanism of erosion. The benefits of nitrogen alloying over surface melting in an inert environment are not substantial, but this may be attributed to pre-existing micro-cracks in the nitrogen alloyed surface layers.

Keywords: Erosion; Water droplets; Laser surface treatment; Ti–6Al–4V

1. Introduction

1.1. Water droplet erosion

Water droplet erosion in the final rows of blading in the low pressure (LP) stage in large steam turbines is the eventual cause of substantial degradation of the blade surface [1]. Partial condensation of water droplets from the superheated steam occurs immediately upstream of the final or penultimate stage of blading in the LP stage. At the very least, erosion degrades the aerodynamic efficiency of the blading and sustained operation ultimately necessitates the costly dismantling and reblading of the turbine.

Ti–6Al–4V alloys currently rival 12Cr martensitic steels for application in the LP stage for two reasons [2]. In the penultimate (L-1) or steam transition row, Ti–6Al–4V may be used because of its high degree of immunity to pitting initiated by corrosive condensates. Failure by corrosion fatigue of 12-Cr blades has historically resulted in substantial downtime. In addition, the high specific strength of the titanium alloy permits longer blade lengths in the last (L-0) row of blading. The associated larger exhaust area results in improved thermal efficiency and a related substantial increase in the power output. Although Ti–6Al–4V demonstrates a relatively high resistance to water droplet attack [3], erosion remains a problem because the longer blades result in increased blade tip velocities.

Conventionally, the leading edge of 12-Cr blades is protected by a brazed Co-based (Stellite) insert. However, thermal expansion mismatch means that this is an inappropriate solution for Ti alloy blading. A range of solutions to the problem are employed by steam turbine manufacturers around the world. Examples include the use of age-hardened β-Ti alloy shields inserted into the leading edge by weld overlay or brazing techniques or TiC-based sintered carbide inserts applied by electron beam welding or brazing. However, a single stage satisfactory process remains elusive. It is to this end that we have examined the effect of laser surface melting in inert and dilute nitrogen atmospheres on the water droplet erosion resistance of Ti–6Al–4V.

1.2. Laser surface alloying

Laser surface treatment has the potential to produce enhanced surface properties in an elegant single stage process. Laser gas alloying (LGA) is such a process, appropriate for producing wear resistant surface layers on Ti alloys. The combined possibilities of precision control and process automation mean that consistent, repeatable results may be obtained, provided that the effects of process variables are thoroughly understood. LGA relies on the rapid, localised melting produced by the intense optical energy of a laser beam. Convection currents in combination with the high dif-

[1] Present address: Department of Materials Science and Metallurgy, Pembroke Street, Cambridge CB2 3QZ, UK.

SSDI 0043-1648(95)07131-8

fusivity of solutes in the liquid state ensure that alloying occurs throughout the melt in the atmosphere of a suitably reactive gas.

In the case of Ti and Ti alloys, surface melting in an atmosphere of N_2 gas results in the formation of a nitrogen rich surface layer. The microstructure of the alloyed region is affected by a range process variables but consists primarily of TiN dendrites within a nitrogen enriched α-Ti matrix [4]. Katayama et al. originally surface melted various Ti alloys in a continuous stream of N_2 gas [5]. They noted the difficulty of producing a smooth, crack-free surface layer. Subsequently, dilutions of N_2 in an inert carrier gas have been considered (eg. [4,6]). Bell et al. have reported that surface cracking can be eliminated by working at high feed rates [7] and more recently, by preheating the substrate prior to laser processing [6]. The previously published work has indicated optimum values for specific variables such as scanning speed, approximate power density and intertrack overlap [6]. This work has therefore utilised the previously published results to produce laser treated surfaces; the water droplet erosion resistance relative to the untreated material has then been evaluated.

2. Experimental techniques

2.1. Laser processing

Laser surface alloying experiments were undertaken at 2 kW using a transverse flow, continuous wave 5 kW CO_2 laser. The beam was focused using a 69° off-axis parabolic mirror with a focal distance of 216 mm. The beam was characterised using a hollow needle beam analyser and the power measured at the workpiece surface using a calibrated calorimeter. Experiments were undertaken below the focal point resulting in an average power density of $\sim 1 \times 10^5$ W cm^{-2}. Because of the minimum depth of melting required for adequate erosion protection, a set traverse velocity of 20 mm s^{-1} was used. All melting occurred in the conduction/convection limited melt regime at the traverse velocity employed.

The gas required for oxidation protection and alloying was delivered via a purpose designed shroud, which included a gas jet aimed directly at the point of interaction between the laser beam and the substrate. The total gas flow was controlled at 20 dm^3 min^{-1} and divided evenly between the gas jet and the shroud system. Three discrete atmospheres were utilised i.e. pure Ar, Ar + 10% N_2 and Ar + 20% N_2 by volume. Surfaces were produced by overlapping adjacent melt tracks. The successive overlap between tracks was either 50% or 75% of the top surface width of the melted region. 50% overlap is the minimum requirement for producing a continuously treated surface layer and the literature has indicated [6] 75% overlap as an optimum for producing an alloyed layer with homogeneous microstructure.

2.2. Water droplet erosion

Specimens were tested in an erosion rig consisting of two contra rotating shafts, each carrying a mild steel overhung disc [8]. The specimens are mounted on the perimeter of the larger diameter disc and the spray nozzles are located on the smaller. The discs are sealed from the atmosphere and the tests conducted under vacuum. Four circular specimens are eroded in any single test by the spray from two nozzles. The 15 mm diameter specimens are machined from the material to be evaluated and the edges protected by replaceable tool steel guard rings. The guard rings ensure that no fragmentation or unrepresentative mass loss occurs from the specimen edges.

Primarily, the water droplet erosion apparatus is intended as a method for the rapid evaluation of the relative erosion resistance of a range of materials. Conditions during testing are, however, designed to approximate the actual operating conditions in the LP stage of a steam turbine. The mean droplet size has been determined, using photographs of the spray, to be approximately 100 μm. The impact velocity of ~ 500 m s^{-1} is well into the regime of impact velocities under which the wear mechanism is dominated by erosion alone [9].

Testing was undertaken in continuous 5 h runs, separated by measurements for mass loss as well as scanning electron microscopy examination of the eroded surface. In any set of four specimens, a comparator was included. The comparator was manufactured from the untreated Ti–6Al–4V and the surface ground to a standard finish. This allowed for an evaluation of the relative performance of the laser treated material as well as maintaining a consistent standard throughout.

3. Results

3.1. Initial microstructure

A detailed analysis of the effect of laser treatment on the initial microstructure is beyond the scope of this work, however a brief discussion is directly relevant to the resultant erosion performance. Prior to laser treatment, the Ti–6Al–4V consists of a predominantly α phase microstructure containing a lower fraction of distributed β phase. Laser melting in an inert atmosphere resulted in a homogeneous martensitic (α′) microstructure to a depth of ~400 μm. Laser melting in dilute nitrogen resulted in a continuous TiN surface layer (5–20 μm thick) covering a relatively inhomogeneous melt zone comprising TiN dendrites, TiN plates, α, and α′ phases.

Pre-existing micro-cracks were evident in all material laser melted in nitrogen containing atmospheres. Crack directions were predominantly either perpendicular or parallel to the direction of the laser tracks. Cross-sectional examination indicated that the cracks were approximately perpendicular to the top surface and penetrated to the depth of the melt zone.

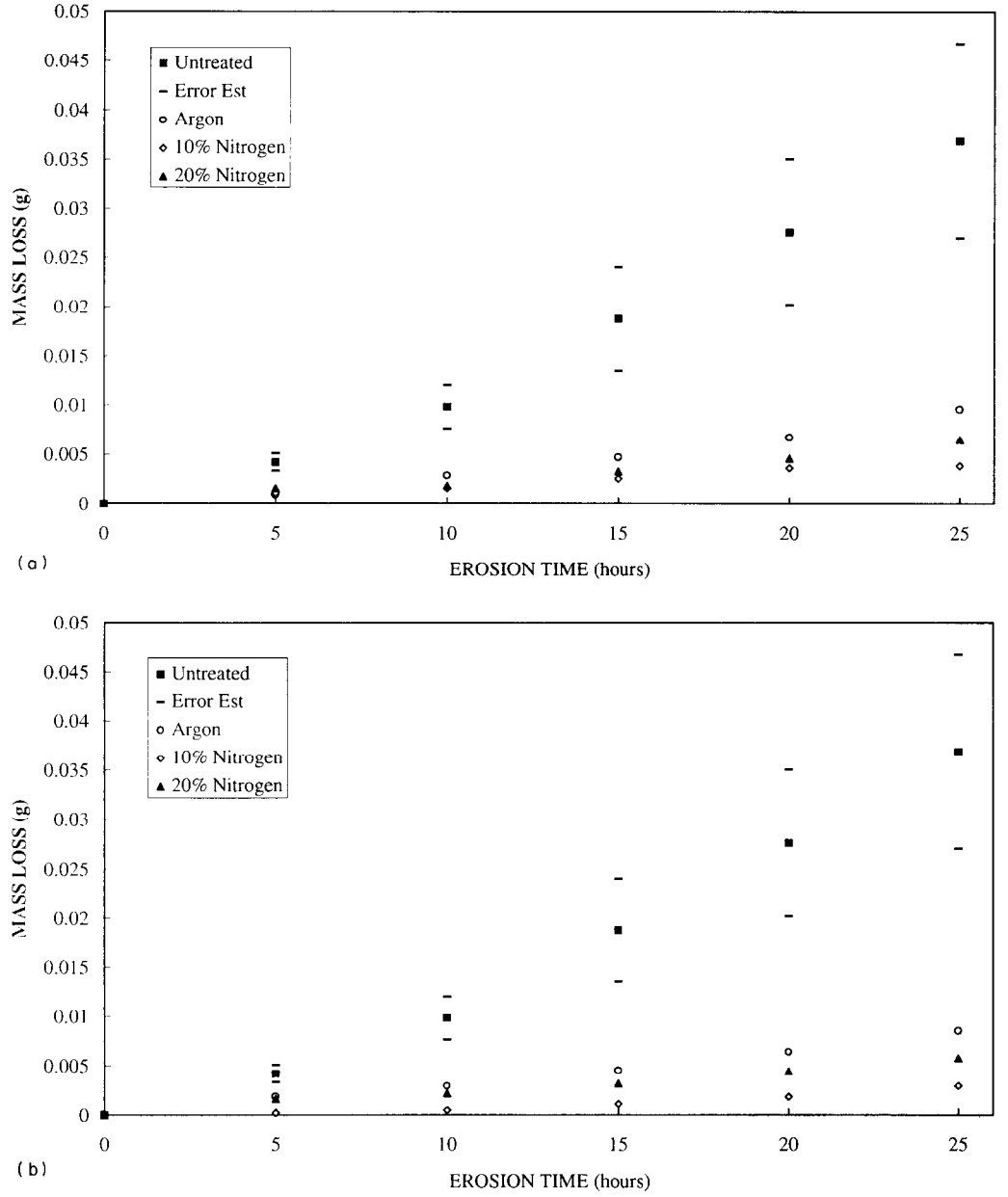

Fig. 1. Water droplet erosion of laser processed Ti–6Al–4V: (a) 50% intertrack overlap; (b) 75% intertrack overlap.

Cracking could not be correlated with specific microstructural features using either optical or scanning electron microscopy.

The Knoop microhardness (50 g load) of the untreated material is 382. Laser melting in argon with either 50% or 75% overlap results in a moderate ($\leq 10\%$) increase where as melting in nitrogen results in a more dramatic ($\sim 40\%$) increase to ~ 550. These figures refer to an average value within the melt zone and do not include the particularly hard surface layer of TiN (hardness ≥ 1200).

3.2. Water droplet erosion

The mass loss during water droplet erosion of Ti–6Al–4V is plotted in Fig. 1 and can be compared to the same material after laser surface melting in both inert and reactive atmospheres. The figure shows the cumulative mass loss vs. time at five hour intervals over 25 h. Fig. 1(a) plots mass loss of material laser treated with 50% overlap and Fig. 1(b), material laser treated with 75% overlap. There is little overall difference between the data in Fig. 1(a) and Fig. 1(b) suggesting that, within the range examined, intertrack overlap is a relatively insignificant parameter.

3.3. SEM examination

Examination of the wear surfaces and wear surface cross-sections can be expected to elucidate the mechanisms of material removal. Fig. 2 shows the eroded wear surfaces after 5 h and Fig. 3 after 25 h exposure to water droplet erosion. It is apparent from Fig. 2 that the erosive attack is non-uniform in

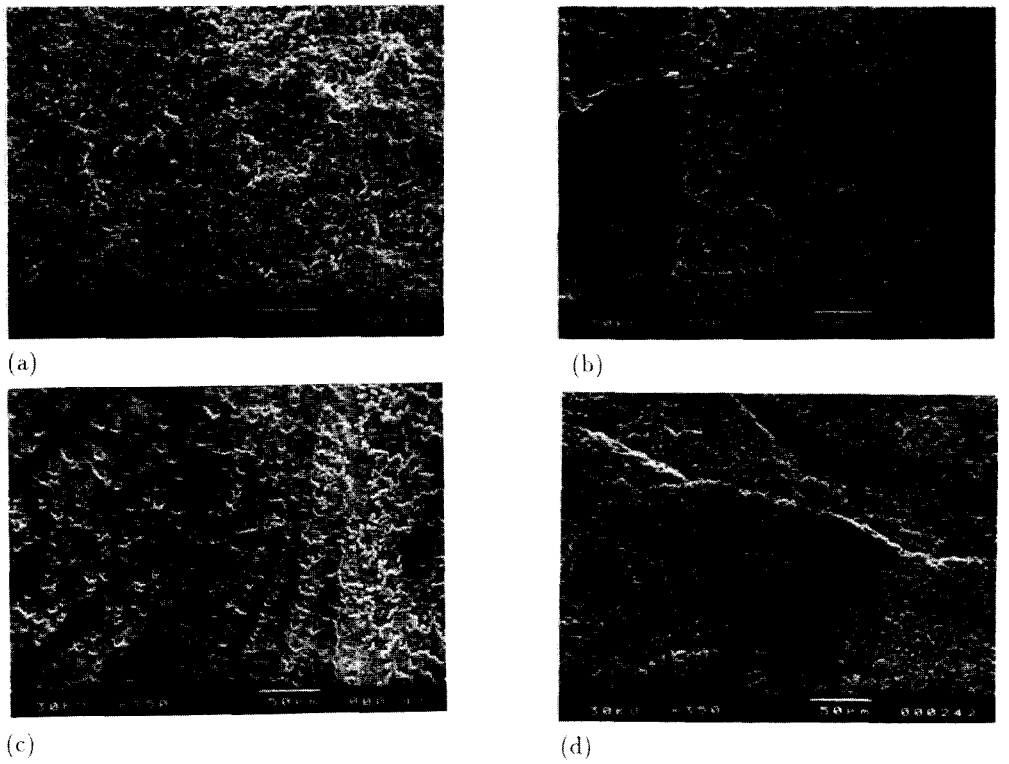

Fig. 2. Secondary electron SEM micrographs of the wear surfaces after 5 h exposure to water droplet erosion: (a) untreated; (b) laser processed in 100% Ar; (c) laser processed in 10% N_2; (d) laser processed in 20% N_2. The direction of laser traverse is vertical in all cases.

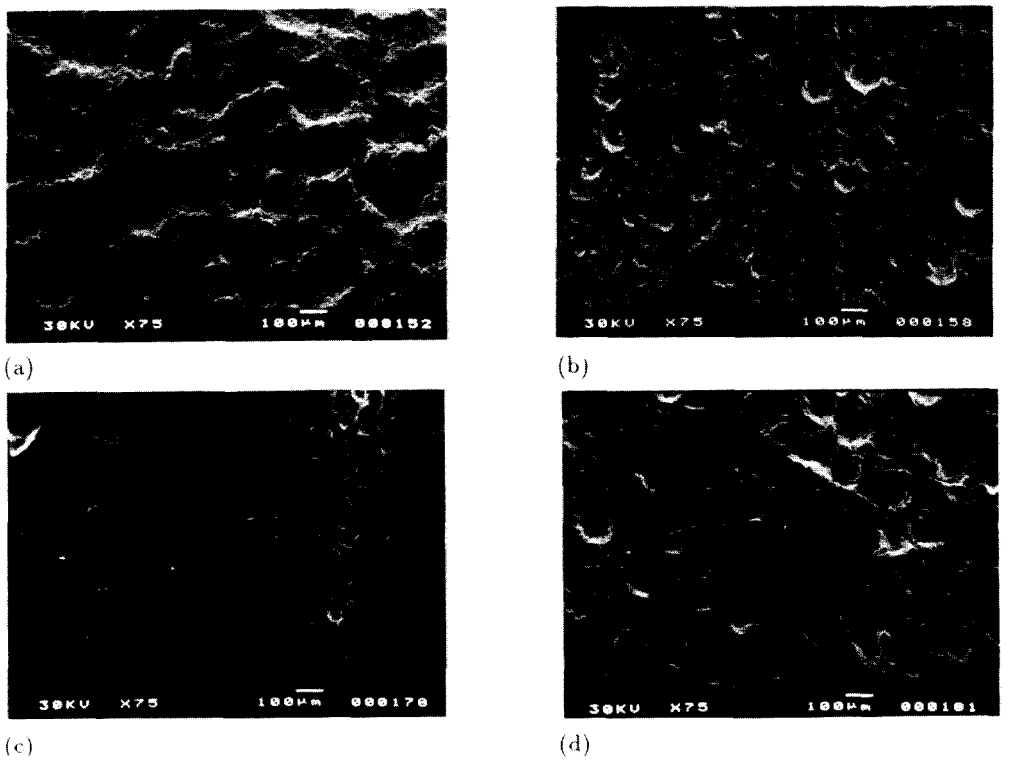

Fig. 3. Secondary electron SEM micrographs of the wear surfaces after 25 h exposure to water droplet erosion: (a) untreated; (b) laser processed in 100% Ar; (c) laser processed in 10% N_2; (d) laser processed in 20% N_2. The direction of laser traverse is vertical in all cases.

all cases. By the end of the first 5 h exposure, approximately 50% of the surface area of untreated Ti–6Al–4V exhibited erosion pits. In the case of all laser treated material, the initial attack was macroscopically characterised by banding, correlated with the laser tracks.

The mechanism of material removal in the untreated material is apparently one of initial pit formation followed by subsurface lateral tunnel formation. This process of material loss is illustrated in the left-hand micrograph in Fig. 4(a). Moreover, the right-hand micrograph in Fig. 4(a) suggests

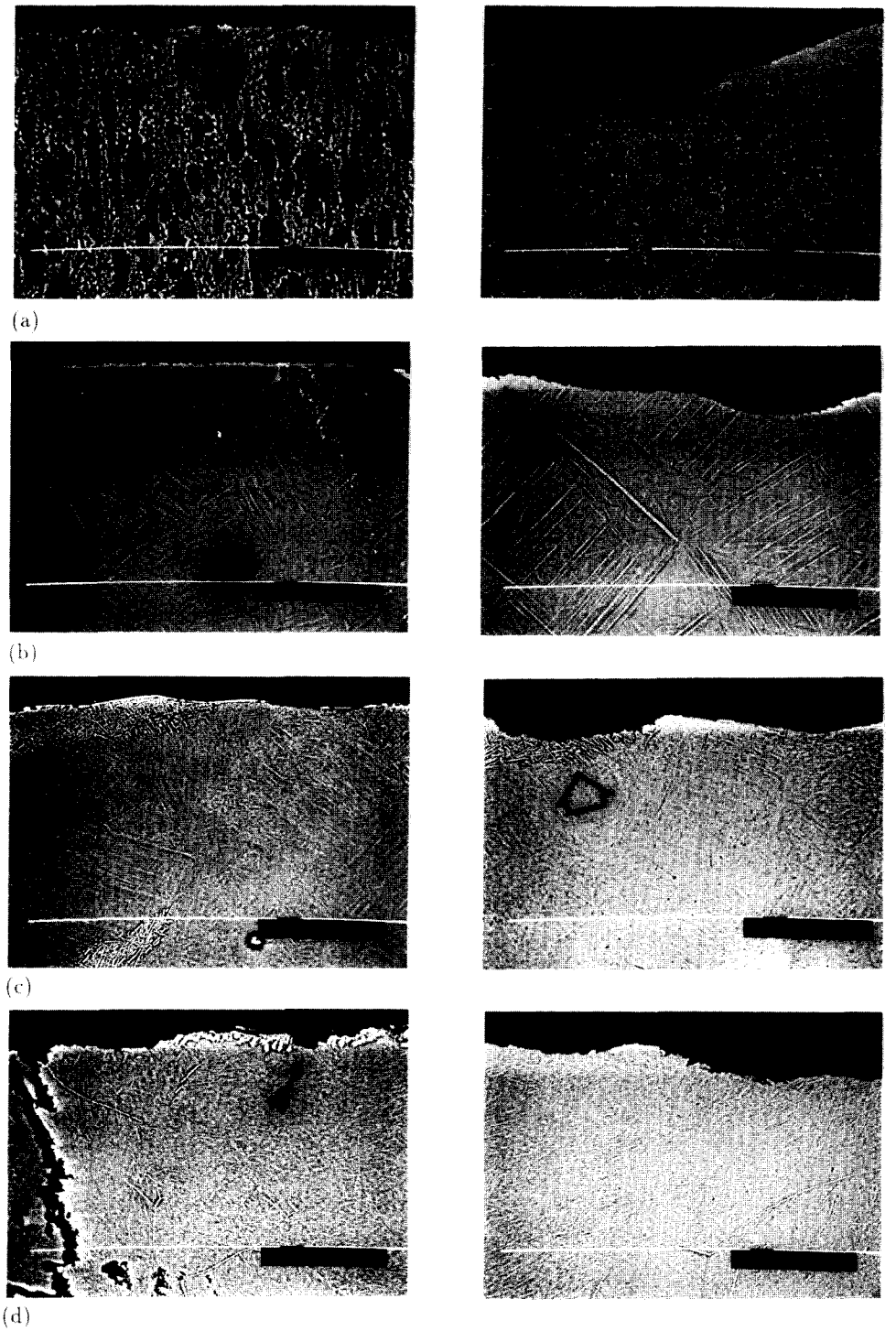

Fig. 4. Backscattered electron SEM micrographs of the erosion surface cross-sections of Ti-6Al-4V, untreated and laser processed with a 50% overlap in 100% Ar, 10% N_2 and 20% N_2 atmosphere. (a) Untreated. After 5 h erosion (left) and after 25 h erosion (right). (b) Laser surface melted in 100% Ar. After 5 h erosion (left) and after 25 h erosion (right). (c) Laser surface melted in 10% N_2. After 5 h erosion (left) and after 25 h erosion (right). (d) Laser surface melted in 20% N_2. After 5 h erosion (left) and after 25 h erosion (right).

that formation of the ~100 μm diameter surface craters occurs by localised attack via the same mechanism.

3.3.1. Surface melting in Ar

For material melted in Ar, the initial erosive attack consisted of a combination of grain boundary erosion and surface roughening or localised erosion pit ($\phi \approx$ 10–50 μm) formation. Roughened bands on the surface were observed to broaden into the adjacent pitted regions as the erosion process developed until the surface assumed a more uniformly eroded appearance. After 15 h exposure to erosion, the banded erosion pattern was less clear than after the initial five hour period and the surface exhibited an approximately uniformly roughened appearance with some local pitting at a developed stage (cratering). Higher magnification examination indicated that the banding is a result of less developed erosion in thin (50–100 μm wide) [2] parallel regions interspersed by more heavily eroded strips (~400 μm wide) [2]. The macroscopic pattern of erosion developed within the first 5 h is therefore maintained. However, no crater or tunnel formation occurred within the initial five hour erosion period. 25 h exposure resulted in a surface dominated by fine roughening and extensive cratering ($\phi \approx$ 100 μm). Limited subsurface tunnel formation was evident; where this occurred, the origin was the base of a surface crater.

Cross-sectional examination indicates that the initial attack is approximately uniform, consistent with the underlying microstructural uniformity. Small pit formation occurs but the lack of subsurface tunnel formation suggests that the martensitic lath microstructure may be more resistant to the lateral propagation of subsurface erosion than the untreated material. After 25 h exposure to erosion, cross-sectional examination confirms that small tunnel formation occurs but subsurface branching is not observed.

3.3.2. Surface melting in 10% N_2

A significant portion of the wear surface of the material melted in 10% N_2 maintains its surface integrity after 5 h exposure to erosion. Surface layer removal is concentrated in narrow (~50 μm wide)[2] bands interspersed by regions decorated with fine ($\phi \approx$ 2–10 μm) erosion pits. Development of the erosion process is facilitated by an increase in the area of the pits, without a concurrent increase in depth. Initiation of this surface layer removal was observed to be locally enhanced in the vicinity of surface cracks. After 15–25 h exposure to erosion, the process of surface layer removal was complete except for in isolated resistant regions. Some cratering ($\phi \approx$ 50–100 μm) was observed to have developed within the narrow banded regions which had suffered the initially more severe attack.

[2] In the case of material melted using 50% overlap.

3.3.3. Surface melting in 20% N_2

Material melted in 20% N_2 exhibited similar characteristics to material melted in 10% N_2. Localised breakdown of the surface layer occurred and was emphasised in the vicinity of pre-existing surface cracks. Heavily eroded regions of the surface exhibited almost complete removal of the surface layer after the initial 5 h exposure to erosion. Heavy cratering of the surface was apparent after exposure to 15 h erosion and some tunnel formation was evident. Orthogonal short (20–75 μm) cracks were also occasionally evident, emanating from the rims of some surface craters. The direction of the cracks matched with the larger cracks present prior to processing i.e. primarily parallel and perpendicular to the direction of laser tracks.

Cross-sectional examination of laser nitrided material indicated that the initial erosive attack comprised of the removal of the brittle TiN surface layer. Micrographs in Fig. 4(c) and (d) illustrate the localised removal of the thin surface layer. This supports evidence from SEM observations of the wear surface which suggest that the initial attack occurred by local removal of the surface layer followed by the approximately uniform spreading of the erosive attack over the specimen surface. Cross-sections of erosion samples after 25 h exposure indicated that total removal of the TiN surface layer was complete. Material melted in 10% N_2 demonstrated a more uniform profile with localised attack favoured in regions of coarser microstructure. Heavy cratering and deep (30 μm) tunnel formation was evident in the case of material melted in 20% N_2.

4. Discussion

The alloy Ti–6Al–4V has been previously observed to demonstrate particularly high water droplet erosion resistance relative to other structural alloys [1]. The results of the present work indicate that laser surface treatments have resulted in an encouraging improvement with reference to the production of erosion resistant surfaces on Ti–6Al–4V turbine blading. An analysis of this performance requires an attempt to define the mechanism of material loss (erosion) in the untreated material and how this is affected by the microstructural changes induced by laser surface treatment. In this regard, recent research [10] correlating the water droplet erosion resistance of pure Ti and a range of Ti alloys suggests a good correlation between Vickers hardness and erosion resistance of the alloys.

The loss of material due to liquid impingement erosion characteristically comprises up to five time-dependent stages (periods) [3]. However, not all stages are necessarily present under all test conditions. The lack of a defined incubation period may occur under conditions of particularly severe impact and the lack of a terminal (steady-state) period may result from a continuing increase in—alternatively, ongoing fluctuations in—the erosion rate. Erosion experiments under-

taken in the present work were unable to resolve either a defined incubation period in the rate of mass loss vs. time nor the onset of a terminal steady state period (constant rate of mass loss). The lack of a defined incubation period is almost certainly the result of the severity of the water droplet erosion under the testing conditions employed. Particularly severe erosion conditions can be expected to result in material removal from the onset of testing, thereby obscuring the incubation stage of erosion (which is characterised by surface deformation with no material removal [1]). In this regard, detailed measurement of mass loss within the first 5 h could be expected to define the incubation period, however short. Recent cavitation erosion experiments [11] on the same material demonstrated a defined incubation period for both untreated Ti–6Al–4V and the same alloy laser surface melted in argon. However, for nitrogen alloyed material the lack of an incubation period was attributed to the early erosion of the continuous brittle TiN surface layer under cavitation conditions.

Longer testing times under the same erosion conditions reported in this work have demonstrated the onset of steady state erosion for untreated Ti–6Al–4V after 25–30 h exposure [12]. The data presented in this work can therefore be used as a useful indication of the potential effectiveness of the laser surface treatments and this can be correlated with changes in the surface-layer microstructure. However it is important to emphasise that the data is insufficient to determine the relative erosion resistance of the laser surface treated samples relative to the bulk under steady-state erosion conditions.

A mechanism of localised damage followed by the nucleation of erosion pits and subsequent development of erosion tunnels from these pits has been previously reported for Ti–6Al–4V [13]. Progressive sectioning of the samples indicated subsurface tunnelling, which was proposed to arise from a hydraulic penetration mechanism initiating within the erosion pits. In the experiments reported in the present work, 5 h exposure to erosion was sufficient to have initiated subsurface tunnel formation below an approximately uniformly eroded surface in the case of untreated material (see Fig. 4(a)). The features observed were therefore consistent with an erosion mechanism dominated by hydraulic penetration at local damage sites. Hydraulic penetration is acknowledged to be the most damaging mode for material removal for two reasons. It has the capacity to substantially develop submicron sized cracks and pits and moreover, it is effective throughout the erosive process. The development of erosion pits to the size of $\phi \geq 100$ μm (craters) was observed to occur by a similar localised mechanism within the craters (see Fig. 4(a)). The development of the erosion process until the end of the test period resulted from an increase in the size of the surface craters as well as the development of large diameter (100–200 μm) tunnels from within these craters.

A rationalisation for the enhanced erosion resistance of the laser melted material should at least consider the microhardness of the melted layer as well as the surface features and cross-sections of the eroded samples. Knoop microhardness tests indicate that material melted in Ar exhibits a marginally increased ($\sim 10\%$) microhardness within the melt zone compared to the bulk. An approximate calculation based on data for the erosion rate dependence on hardness of a range of titanium alloys [10] shows that a 10% increase in hardness can be expected to produce a relative erosion resistance of ~ 1.3. The ratio of the steady state erosion rate of laser surface melted (100% Ar, overlap $\approx 25\%$) Ti–6Al–4V relative to that of the untreated material has been previously measured to be ~ 1.7 [12] (under the same erosion conditions as the present work). The experiments reported in the present work (100% AR, overlap $\geq 50\%$) show a decrease in the rate of mass loss relative to the previous data and therefore suggest that further improvements to the steady-state relative erosion resistance would become evident over longer testing times. Microstructural evidence from examination of the erosion surface cross-section indicates why an improvement over and above that expected from microhardness data may arise. Small subsurface erosion tunnels readily develop from the surface of the material. However, the tunnels observed do not develop orthogonal branches (see Fig. 4(b)). This microstructural evidence suggests that the hydraulic penetration mechanism of erosion may be constrained by the martensitic lath microstructure. Further evidence for this hypothesis comes from a consideration of a cavitation erosion evaluation [11] of the same material. Under cavitation erosion conditions, the steady state erosion rate of Ti–6Al–4V was not improved by laser surface melting. Cross-sectional examination showed that subsurface tunnel formation did not occur i.e. hydraulic penetration was not the operative mechanism in this case. The mechanism of material removal under cavitation erosion was rather one of the accumulation of plastic deformation and subsequent spalling off of the surface. The martensitic microstructure was therefore not particularly advantageous in the case of cavitation erosion.

In the case of material melted in nitrogen, the continuous surface layer of TiN acts as an initial barrier to erosion. The mechanism of material loss is one of local pitting of the brittle TiN surface layer and increased local spalling off of the TiN in the vicinity of cracks. In the case of material melted in a 20% N_2 atmosphere, a higher density of cracks is therefore likely to contribute to the increased initial rate of material loss. Nitrogen alloying in all cases (10 and 20% N_2, 50 and 75% overlap) resulted in a substantial increase ($\sim 40\%$) in the microhardness of the melted layer matrix relative to the untreated Ti–6Al–4V. This alone can be expected to contribute to an improved erosion resistance. However, it is important to consider the relative inhomogeneity of the microstructure of the material melted in dilute nitrogen atmospheres relative to that melted in an inert atmosphere. Microstructural inhomogeneity in nitrogen alloyed material was observed to influence the local erosive attack in that regions of coarse microstructure were more vulnerable to erosion through local attack of the softer phase (see Fig. 4(c)). It is likely therefore, that the inhomogeneity of the microstructure in conjunction with the pre-existing

micro-cracks resulted in a less dramatic improvement in erosion resistance than the hardness increases may have indicated.

5. Conclusions

1. The experiments presented in this work have demonstrated the potential benefits of laser surface melting and nitrogen alloying on the water droplet erosion resistance of Ti–6Al–4V. Melting in both inert and dilute nitrogen atmospheres results in a substantial decrease in mass loss during exposure to water droplet erosion relative to untreated Ti–6Al–4V.
2. In the case of material melted in argon, the improved resistance to water droplet erosion can be attributed to a combination of increased hardness in combination with the effect of the martensitic microstructure on the hydraulic penetration mechanism of erosion.
3. For Ti–6Al–4V laser alloyed with nitrogen, the explanation is apparently less straightforward. Initially, the brittle TiN layer acts as a barrier to the onset of erosion damage. However, the non-uniformity of the microstructure in combination with pre-existing cracks influence the erosion mechanism, making it more difficult to rationalise the observed behaviour. Further experiments on material without pre-existing cracks and, ideally, with a more homogeneous microstructure are necessary.
4. It is imperative that methods are devised to eliminate micro-cracking which occurs within the laser treated surface layers; such cracking is likely to have an effect on the fatigue resistance of the surface treated component. Even if cracking does not occur, methods to minimise the tensile residual stresses which exist in the melted surface layer must be devised. The use of a two stage laser treatment to anneal the melted layer may hold some promise in this regard.

Acknowledgements

The authors are grateful to Mr E. Tate and colleagues of the Materials Engineering Department, Parsons Steam Turbines Ltd for useful discussions and technical support. In addition, the support of Parsons for the supply of material as well as the provision of water droplet erosion test facilities is acknowledged. Primary financial support for the work from the Science and Engineering Research Council (Grant ref. GR/H 36535) is also acknowledged. We are particularly grateful to professor D.R.F. West for useful discussions and enthusiastic support of the work. Professor M. McLean is thanked for the provision of research facilities at Imperial College.

References

[1] J.H. Brunton and M.C. Rochester, Erosion of solid surfaces by the impact of liquid drops, in C.M. Preece (ed.), *Treatise on Materials Science and Technology*, Vol. 16, Academic Press, New York, 1979, pp. 185–248.
[2] R.I. Jaffee, Titanium steam turbine blades, *J. Mater., 41* (3) (1989) 31–35.
[3] F.J. Heyman, Liquid impingement erosion, in *Wear, ASM Handbook*, Vol. 18, ASM, 1992, pp. 221–232.
[4] B.L. Mordike, Laser gas alloying, in C.W. Draper and P. Mazzoldi (eds.), *Laser Surface Treatment of Metals, San Miniato, Italy, September 1985*, Martinus Nijnhoff, Dordrecht, 1985, pp. 389–412.
[5] S. Katayama, A. Matsunawa, A. Morimoto, S. Ishimoto and Y. Arata, Laser nitriding of titanium and its alloys, *Proc. 3rd Int. Colloq. on Welding and Melting by Electron and Laser Beam, Lyon, France, September 1983*, CEN, Saclay, 1983.
[6] P.H. Morton, T. Bell, A. Weisheit, J. Kroll, B.L. Mordike and K. Sagoo, Laser gas nitriding of titanium and titanium alloys, in T.S. Sudarshan and J.F. Braza (eds.), *Surface Modification Technologies*, Vol. 5, 1992, pp. 593–609.
[7] T. Bell, H.W. Bergmann, J. Lanagan, P.H. Morton and A.M. Staines, Surface engineering of titanium with nitrogen, *Surf. Eng.*, 2 (1986) 133–143.
[8] A. Smith, R.P. Kent and R.L. Armstrong, Erosion of steam turbine blade shield materials, in *Erosion by Cavitation or Impingement, ASTM Spec. Tech. Publ. 408*, ASTM, Philadelphia, PA, 1967.
[9] P.A. Coulon, Erosion–corrosion in steam turbines II: A problem largely resolved, *Lubr. Eng., 42* (1986) 357–362.
[10] N. Yasugahira, K. Namura, R. Kaneko and T. Satoh, Erosion resistance of titanium alloys for steam turbines blades as measured by water droplet impingement, in *Titanium Steam Turbine Blading, Palo Alto, 1988*, Pergamon, New York, 1990, pp. 385–401.
[11] J.M. Robinson, S. Anderson, R.D. Knutsen and R.C. Reed, Cavitation erosion of laser melted and laser nitrided Ti–6Al–4V, *Mater. Sci. Technol.*, to be published.
[12] NEI Parsons, Ltd., unpublished test results, April 1991.
[13] W.F. Adler, The mechanics of liquid impact, in C.M. Preece (ed.), *Treatise on Materials Science and Technology*, Vol. 16, Academic Press, New York, 1979, pp. 127–183.